Theory of surface effects in binary alloys. IV. Ordering alloys with two ferromagnetic components

Jesús Urías
Instituto de Física, Universidad Autónoma de San Luis Potosí, San Luis Potosí, San Luis Potosí, México

J. L. Morán-López
Departamento de Física Centro de Investigación y de Estudios Avanzados del Instituto Politecnico Nacional, Apartado Postal 14-740, México 14, Distrito Federal, México

(Received 23 June 1980)

A theory of the surface concentration, spatial long-range order and magnetism for binary body-centered-cubic ordering alloys with ferromagnetic components is presented. It is a mean-field theory based on a model consisting of pairwise interactions between nearest neighbors only. We find that for an alloy A_xB_{1-x} with spins S_A, S_B and Ising exchange integrals J_{AA}, J_{AB}, and J_{BB}, magnetism favors surface segregation of the I component if $S_I^2 J_{II} < S_{I'}^2 J_{I'I'}$ $(I,I'=A,B)$. Results for the surface concentration and the long-range order parameters at $T=0$ are presented. At finite temperatures, alloys with several bulk behaviors are studied, i.e., (i) T_0 (spatial order-disorder critical temperature) $< T_M$ (Curie temperature), (ii) $T_0 > T_M$, and (iii) $J_{AB} << J_{AA}, J_{BB}$. It is found that in case (iii) there is a range of temperatures where the surface is magnetic whereas the bulk is paramagnetic. Also studied is the effect on the surface properties produced by allowing the chemical and magnetic interactions to be location dependent. It is found in general that the results are more sensitive to changes in the chemical interactions. The FeCo system is examined along these lines, and the results are compared with existing experimental data.

I. INTRODUCTION

In recent publications, we have studied surface effects for the two different kind of binary alloys, ordering[1] and clustering,[2] hereafter referred as Papers I and II. In those reports we were mainly concerned with the interplay of surface segregation and spatial order. Papers I and II included short- and long-range order simultaneously in order to describe the system properly over the whole range of temperatures. An extension to Paper I to study the surface effects at stepped body-centered-cubic ordering alloys has been outlined in the preceding paper.[3]

All the previous theories are valid for nonmagnetic systems or for ferromagnets at temperatures above the Curie temperatures where the system becomes paramagnetic. Phenomena equally important to those mentioned above are the magnetic properties near the surface of binary alloys with either one or two ferromagnetic components. In these systems the magnetization at the surface may differ from that in the bulk not only because of the reduction in the coordination number but also because of differences in the chemical composition and degree of spatial order.[4,5]

The interdependence of magnetism and spatial long-range order, in the bulk, is experimentally[6,7] well established. However, because of the inherent complexity of the problem, theoretical analyses are usually carried out ignoring one or the other effect.[8,9] Recently it has been shown[10,11] that in alloys with two magnetic species the interplay of the two phenomena may lead to results completely different from those predicted by theories that take into account only one of the effects. At the surface the complexity is increased due to the segregation phenomena. Then, to study surface effects in magnetic alloys, spatial order, segregation, and magnetism have to be treated on equal footing.

In this paper we study these phenomena within the mean-field (Bragg-Williams) approximation; i.e., taking into account only long-range-order effects. The interatomic forces are assumed to be pairwise between nearest neighbors only. The magnetic interactions are of the Ising type and restricted also to nearest neighbors. We study in detail the interplay between atomic order and ferromagnetism at the surface of ferromagnetic alloys with several bulk behaviors.

In Sec. II the bulk properties are summarized. The calculation for the surface phenomena is outlined in Sec. III and the general results as well as those for the FeCo system are discussed in Sec. IV.

II. BULK PROPERTIES

The formalism employed in the theoretical analysis for the bulk is described in detail in Ref. 11. Here we summarize only some of the main features.

We consider a body-centered-cubic binary alloy A_xB_y (where $x+y=1$) with spins S_A and S_B. The contributions to the total energy are the chemical nearest-neighbor interactions U_{AA}, U_{AB}, and U_{BB} and the Ising exchange integrals J_{AA}, J_{AB}, and J_{BB} (defined positive for ferromagnetic coupling).

At low temperatures, alloys tend either to develop spatial long-range order (ordering alloys) or to separate into two phases (segregating alloys). In our model this behavior is governed by the sign of the effective "heat of mixing,"

$$W_{\text{eff}} = W_C + W_M \ . \tag{2.1}$$

If $W_{\text{eff}} > 0$ the system orders spatially into an A-B-A-B—type system; if $W_{\text{eff}} < 0$ the system segregates into two separate A-A and B-B subsystems.

The chemical (W_C) and magnetic (W_M) contributions to the heat of mixing are defined by

$$W_C \equiv U_{AA} + U_{BB} - 2U_{AB} \ , \tag{2.2}$$

$$W_M \equiv 2S_A S_B J_{AB} - S_A^2 J_{AA} - S_B^2 J_{BB} \ . \tag{2.3}$$

Here we restrict ourselves to ordering alloys ($W_{\text{eff}} > 0$). In order to describe the spatial long-range order, we consider a bcc lattice which is subdivided into two equivalent sublattices, α and β. All α sites have β sites as nearest neighbors and vice versa. In the perfectly ordered case of the $A_{0.5}B_{0.5}$ alloy, all α sites are occupied by A atoms and all β sites by B atoms. In the disordered case the probabilities of finding an A atom in the α and β sublattices are the same.

To describe the magnetic properties of the system we define the probabilities $p_\nu(Im)$ of finding an atom I ($I=A,B$) with spin $S_z = m$ ($-S_I \le m \le S_I$) in the sublattice ν ($\nu=\alpha,\beta$). For the sake of definiteness and simplicity we choose $S_A = S_B = \frac{1}{2}$; therefore $m = \uparrow, \downarrow$ and there are eight distinct p_ν's. The probabilities are normalized by

$$p_\nu(A\uparrow) + p_\nu(A\downarrow) + p_\nu(B\uparrow) + p_\nu(B\downarrow) = 1 \qquad (\nu=\alpha,\beta) \tag{2.4}$$

and the average concentration x of species A is given by

$$\tfrac{1}{2}[p_\alpha(A\uparrow) + p_\alpha(A\downarrow) + p_\beta(A\uparrow) + p_\beta(A\downarrow)] = x \ . \tag{2.5}$$

The equilibrium values for the probabilities are found by minimizing the free energy $F = U - TS$, subject to the three constraints (2.4) and (2.5). Five free parameters are chosen as linear combinations of the eight probabilities $p_\nu(Im)$.

We define a chemical long-range order parameter

$$\eta \equiv [p_\alpha(A\uparrow) + p_\alpha(A\downarrow)] - [p_\beta(A\uparrow) + p_\beta(A\downarrow)] \tag{2.6}$$

and four magnetic long-range order parameters

$$\xi_\nu(I) \equiv p_\nu(I\uparrow) - p_\nu(I\downarrow) \ . \tag{2.7}$$

In terms of these order parameters the internal energy can be written

$$U \equiv U_C + U_M \ , \tag{2.8}$$

where

$$U_C(\eta) = U_C(0) - \tfrac{1}{8} NZ W_C \eta^2 \tag{2.9}$$

and

$$U_M = -\tfrac{1}{8} NZ \sum_{I,I'} \xi_\alpha(I)\xi_\beta(I')J_{II'} \ , \tag{2.10}$$

where N is the total number of atoms and Z is the number of nearest neighbors. The entropy is given by the expression

$$S = -\tfrac{1}{2} kN \sum_{I\nu m} [p_\nu(Im) \ln p_\nu(Im)] \ . \tag{2.11}$$

We now define two basic parameters: an unperturbed Curie temperature Θ_M

$$8k\Theta_M \equiv Z(xJ_{AA} + yJ_{BB}) + Z[(xJ_{AA} - yJ_{BB})^2 + 4xyJ_{AB}^2]^{1/2} \ , \tag{2.12}$$

which is the Curie temperature[8] if $U_C = 0$; and an unperturbed ordering temperature[12] Θ_0

$$k\Theta_0 = ZxyW_C \ , \tag{2.13}$$

which is the ordering temperature if $U_M = 0$.

In the mean-field approximation the concentration dependence of the Curie temperature Θ_M of a disordered ferromagnet can show five different behaviors. Without loss of generality we choose $J_{AA} < J_{BB}$ and therefore $\Theta_M(x=0) > \Theta_M(x=1)$ for all five cases.

(i) If there is no magnetic ordering energy, i.e., $J_{AB} = \frac{1}{2}(J_{AA} + J_{BB})$, then the Curie temperature shows linear behavior with x:

$$\Theta_M(x) = x\Theta_M(x=0) + y\Theta_M(x=1) \ . \tag{2.14}$$

(ii) If $\frac{1}{2}(J_{AA} + J_{BB}) < J_{AB} < J_{BB}$, then $\Theta_M(x)$ is still a monotonically decreasing function of x, but lies above the line given in (2.14).

(iii) If $J_{AA} < J_{AB} < \frac{1}{2}(J_{AA} + J_{BB})$ then Θ_M, still a monotonically decreasing function of x, lies below the straight line (2.14).

(iv) If $J_{BB} < J_{AB}$ there is a maximum of $\Theta_M(x)$ for $0 < x < 1$.

(v) If $J_{AB} < J_{AA}$ there is a minimum of $\Theta_M(x)$ for $0 < x < 1$.

Cases (ii) and (iv) correspond to a positive ordering magnetic energy, which enhances the chemical ordering energy. Cases (iii) and (v) correspond to negative ordering magnetic energy, i.e., a segregating component that opposes the chemical ordering component.

We consider now three cases:

A. $\Theta_0 < \Theta_M$

At $T=\Theta_M$ there is a second-order transition between a disordered ferromagnet ($T<\Theta_M$) and a disordered paramagnet ($T>\Theta_M$). At a lower temperature T_0 there is, in general, another second-order transition between an ordered ferromagnet ($T<T_0$), and a disordered one ($T_0<T<\Theta_M$). The transition temperature T_0 and $\xi_\alpha(A)=\xi_\beta(A)\equiv\xi_A$ and $\xi_\alpha(B)=\xi_\beta(B)\equiv\xi_B$ at $T=T_0$ are obtained by solving the three coupled equations

$$Z(\xi_A J_{AA}+\xi_B J_{AB})=2kT_0\ln[(x+\xi_A)/(x-\xi_A)] \tag{2.15}$$

and similarly for $A\leftrightarrow B$, $x\leftrightarrow y$; and

$$\tau_0^3+B\tau_0^2+C\tau_0+D=0\ , \tag{2.16}$$

where

$$\tau_0=kT_0/2Z\ , \tag{2.17a}$$

$$B=\tfrac{1}{8}[(x-\xi_A^2)J_{AA}+(y-\xi_B^2)J_{BB}-2\xi_A\xi_B J_{AB}-4xyW_C]\ , \tag{2.17b}$$

$$C=-\tfrac{1}{16}y(x^2-\xi_A^2)[J_{AA}W_C-\tfrac{1}{4}(J_{AA}J_{BB}-J_{AB}^2)]-\tfrac{1}{16}x(y^2-\xi_B^2-\xi_B^2)[J_{BB}W_C-\tfrac{1}{4}(J_{AA}J_{BB}-J_{AB}^2)]\ , \tag{2.17c}$$

$$D=-\tfrac{1}{128}(x^2-\xi_A^2)(y^2-\xi_B^2)(J_{AA}J_{BB}-J_{AB}^2)W_C\ . \tag{2.17d}$$

B. $\Theta_M < \Theta_0$

In this case, there is at $T=\Theta_0$ a second-order Bragg-Williams transition between an ordered ($T<\Theta_0$) and a disordered ($T>\Theta_0$) paramagnet. There is also, in general, a lower temperature T_M at which a second-order transition between an ordered ferromagnet ($T<T_M$) and an ordered paramagnet ($T_M<T<\Theta_0$) occurs. The values of T_M and η at $T=T_M$ are given by the solution of the coupled equations

$$ZW_C\eta=kT_M\ln\frac{(2x+\eta)(2y+\eta)}{(2x-\eta)(2y-\eta)} \tag{2.18}$$

and

$$(2kT_M/Z)^4-\tfrac{1}{16}[(4y^2-\eta^2)J_{BB}^2+(4x^2-\eta^2)J_{AA}^2+(8xy+2\eta^2)J_{AB}^2](2kT_M/Z)^2+\tfrac{1}{256}(4x^2-\eta^2)(4y^2-\eta^2)\times(J_{AA}J_{BB}-J_{AB}^2)^2=0\ . \tag{2.19}$$

C. $J_{AB} \ll J_{AA}, J_{BB}$ and $\Theta_0 < \Theta_M$

In this situation the low-temperature behavior is different from that discussed in Sec. II A. Because of the weak magnetic exchange between dissimilar atoms the system becomes paramagnetic at the temperature T_M' where the chemical order is strong, and becomes ferromagnetic again at a higher temperature T_M'' where the system is disordered enough to take advantage of the strong exchange interactions J_{AA} and J_{BB}.

The temperatures T_M' and T_M'' and the corresponding values for the parameter η at those temperatures are obtained from Eqs. (2.18) and (2.19).

III. SURFACE PROPERTIES

In order to study the surface properties we classify the atoms in the crystal according to the (110) planes n they belong to. Plane $n=0$ corresponds to the surface layer. We define then, eight probabilities per plane $p_\nu^n(Im)$. In a similar way to the bulk we define a chemical long-range order parameter

$$\eta_n\equiv[p_\alpha^n(A\uparrow)+p_\alpha^n(A\downarrow)]-[p_\beta^n(A\uparrow)+p_\beta^n(A\downarrow)] \tag{3.1}$$

and four magnetic long-range order parameters

$$\xi_\nu^n(I)=p_\nu^n(I\uparrow)-p_\nu^n(I\downarrow) \tag{3.2}$$

per plane. These probabilities must satisfy also the normalization conditions similar to Eqs. (2.4) and the average concentration in plane n is given by

$$\tfrac{1}{2}[p_\alpha^n(A\uparrow)+p_\alpha^n(A\downarrow)+p_\beta^n(A\uparrow)+p_\beta^n(A\downarrow)]=x_n\ . \tag{3.3}$$

Equations (3.1)–(3.3), together with the relationships for the normalization of the probabilities enable us to write the eight probabilities $p_\nu^n(Im)$ in terms of the concentration x_n and the long-range order parameters η_n and $\xi_\nu^n(I)$. The equilibrium values of the order parameters are obtained by minimizing a trial free energy $F=U-TS$ with respect to them. In the semi-infinite crystal U_C and U_M are given by

$$U_C=\text{const}+\mathfrak{N}W_C\sum_{n=0}^{\infty}\{\tfrac{1}{2}Z_0[x_n^2+x_n(\Delta_C-1)-\tfrac{1}{4}\eta_n^2]+Z_1[x_nx_{n+1}+\tfrac{1}{2}(x_n+x_{n+1})(\Delta_C-1)-\tfrac{1}{4}\eta_n\eta_{n+1}]\} \tag{3.4}$$

and

$$U_M=\frac{-\mathfrak{N}}{8}\sum_{n=0}^{\infty}\left[Z_0\sum_{I,I'}\xi_\alpha^n(I)\xi_\beta^n(I')J_{II'}+Z_1\sum_{\substack{I,I'\\ \nu\neq\nu'}}\xi_\nu^n(I)\xi_\nu^{n+1}(I')J_{I,I'}\right] . \tag{3.5}$$

Here $\mathfrak{N}$ is the total number of atoms per plane, Z_0 is the number of nearest neighbors within the same layer, and Z_1 is the number of nearest neighbors to one atom which are in one of the adjacent layers. The total number of nearest neighbors is $Z=Z_0+2Z_1$. The parameter Δ_C is defined by

$$\Delta_C\equiv\frac{U_{AA}-U_{BB}}{W_C} . \tag{3.6}$$

The entropy is given by

$$S=-\tfrac{1}{2}k\mathfrak{N}\sum_{n=0}^{\infty}\sum_{I\nu m}[p_\nu^n(Im)\ln p_\nu^n(Im)] . \tag{3.7}$$

The equilibrium values for the concentrations x_n are obtained by the condition of chemical equilibrium

$$\frac{\partial F}{\partial x_n}(\text{all other } x_m \text{ constant})=\frac{\partial F}{\partial x}(\text{bulk}) . \tag{3.8}$$

A. Results at $T=0$

At zero temperature, only the surface layer can be, at equilibrium, different from the bulk.[1] If the bulk parameters are x, η, and $\xi_\nu(I)$, only x_0 may be different from x, only η_0 may be different from η, and only $\xi_\nu^0(I)$ may be different from $\xi_\nu(I)$. The values for the long-range order parameters that minimize the free energy for $x_0<\frac{1}{2}$ are

$$\eta_0=2x_0,\quad \xi_\alpha^0(A)=2x_0,\quad \xi_\alpha^0(B)=1-2x_0 ,$$
$$\xi_\beta^0(B)=1,\quad \xi_\beta^0(A)=0 \tag{3.9}$$

and for $x_0>\frac{1}{2}$ are

$$\eta_0=2y_0,\quad \xi_\alpha^0(A)=1,\quad \xi_\alpha^0(B)=0 ,$$
$$\xi_\beta^0(A)=2x_0-1\quad \xi_\beta^0(B)=2y_0 . \tag{3.10}$$

The equilibrium values for x_0 are obtained from Eq. (3.3) the results for x_0 and η_0 are shown in Fig. 1 as a function of

$$\Delta_{\text{eff}}=\frac{\Delta_C W_C-\Delta_M W_M}{W_C+W_M} . \tag{3.11}$$

Here Δ_M is defined by

$$\Delta_M\equiv\frac{S_A^2J_{AA}-S_B^2J_{BB}}{W_M} . \tag{3.12}$$

The values for Δ_1 and Δ_2 depend on the concentration in the bulk and are given by

$$\Delta_1=\begin{cases}-1 , & x<\frac{1}{2}\\ \dfrac{Z-Z_1}{Z_1} , & x=\frac{1}{2}\\ \dfrac{5Z-Z_0}{2Z_1}-4x , & x>\frac{1}{2} ,\end{cases} \tag{3.13}$$

$$\Delta_2=\begin{cases}\dfrac{Z+3Z_0}{2Z_1}+4x , & x<\frac{1}{2}\\ \dfrac{Z-Z_1}{Z_1} , & x=\frac{1}{2}\\ -1 , & x>\frac{1}{2} .\end{cases}$$

In all cases we find that there are three possible situations depending on the value of Δ_{eff}, i.e., (i) $x_0=0$, $\eta_0=0$, (ii) $x_0=\frac{1}{2}$, $\eta_0=1$, and (iii) $x_0=1$, $\eta_0=0$. Cases (i) and (iii) correspond to the situation where the surface is made of atoms of only one species and case (ii) corresponds to a surface layer with equiatomic concentration and completely ordered. It is worth noticing that magnetism would tend to segregate the element I if $S_I^2J_{II}<S_{I'}^2J_{I'I'}$.

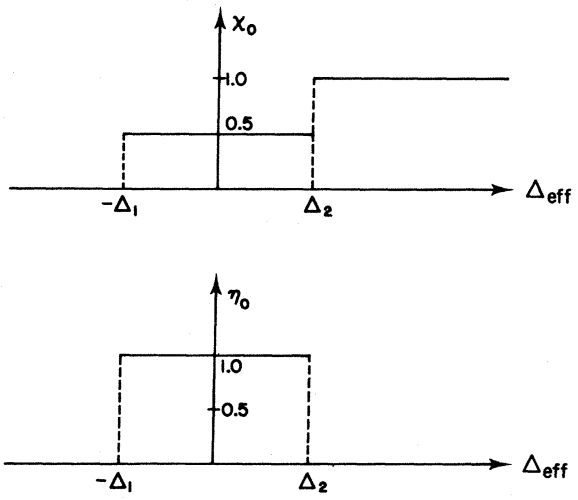

FIG. 1. Surface concentration x_0 and surface long-range order parameter η_0 as functions of Δ_{eff} (see text) at $T=0$. The discontinuities occur at Δ_1 and Δ_2 defined in Eqs. (3.13).

B. $\Theta_0 < \Theta_M$

In Figs. 2–4, we show results for an alloy with Curie temperature higher than the order-disorder critical temperature. An example of this kind of alloys is the Fe_xCo_y system. The phase diagram reported by Hansen,[13] shows a maximum in the Curie temperature ($\Theta_M = 1258$ K) at $x = 0.535$ and a maximum in the spatial order-disorder temperature ($T_0 = 1003$ K) at $x \simeq 0.49$. In a more recent experiment[14] the maximum was found at $T = 998.6$ K and $x \simeq 0.48$. The theory summarized in Sec. II was applied for this system,[11] obtaining in general good agreement with the reported phase diagram. The parameters J_{CoCo}, J_{CoFe}, J_{FeFe}, and W_C were obtained from the three experimental values of the Θ_M at $x = 0.4$, 0.5, and 0.6 and from T_0 at $x = 0.5$. The values for U_{CoCo} and U_{FeFe} were obtained from the cohesive energy of the pure elements. They are in absolute units $J_{CoCo} = 393.77$, $J_{FeCo} = 805.473$, $J_{FeFe} = 497.92$, $W_C = 387.07$, $U_{CoCo} = -50\,908.94$, and $U_{FeFe} = -49\,783.31$. With these values we obtained $\Delta_C = 2.91$, $\Delta_M = 0.145$, and $\Delta_{eff} = 1.94$.

In Fig. 2 we present results for the temperature dependence of x_0 for several values of x. We show in Fig. 3 the results for η_0, η, $\bar{\xi}$, and $\bar{\xi}^0$ as functions of temperature for the same set of values. Here, $\bar{\xi}$ and $\bar{\xi}^0$ are defined by

$$\bar{\xi} = \frac{1}{2}\sum_{l,\nu} \xi_\nu(l), \quad \bar{\xi}^0 = \frac{1}{2}\sum_{l,\nu} \xi_\nu^0(l) \ . \tag{3.14}$$

Figure 4 contains the results for the temperature dependence of ξ_α^0(Fe), ξ_β^0(Fe), ξ_α^0(Co), and ξ_β^0(Co), for values of x used in Figs. 2 and 3.

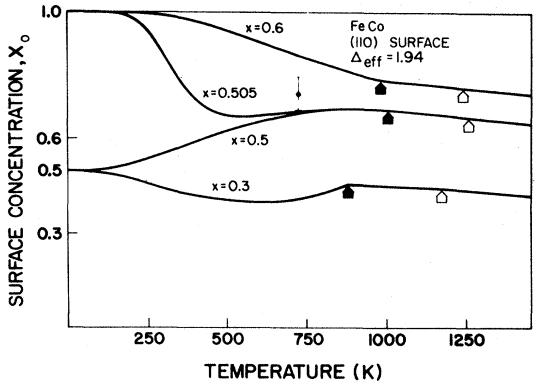

FIG. 2. Surface concentration x_0 as a function of temperature for the (110) face of a bcc material and for various values of x. The open and the solid arrows mark the transition temperatures T_0 and T_M for the corresponding x. The parameters taken correspond to the Fe_xCo_{1-x} system. The experimental results (Ref. 15) are shown by the bar at $T = 725$ K.

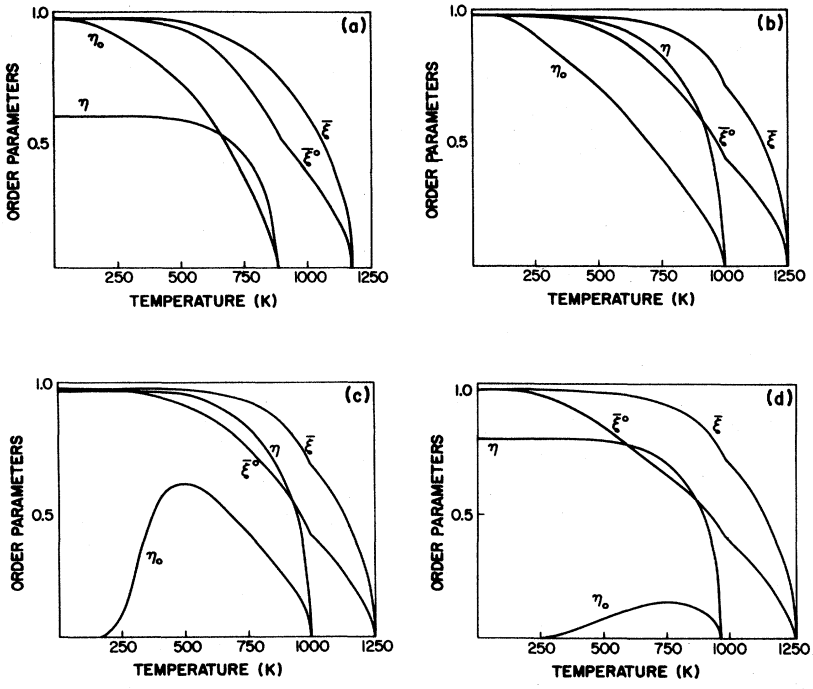

FIG. 3. Surface and bulk long-range order parameters η_0 and η and average magnetizations $\bar{\xi}^0$ and $\bar{\xi}$ as functions of temperature for the same set of values as those in Fig. 2 with concentration $x = 0.3$ (upper left), $x = 0.5$ (upper right), $x = 0.505$ (lower left), and $x = 0.6$ (lower right).

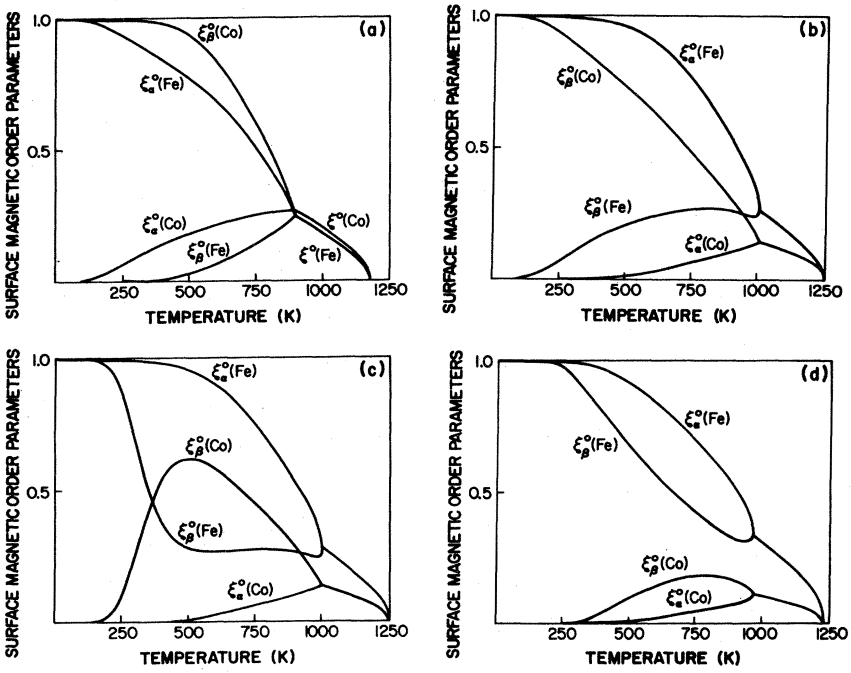

FIG. 4. Surface magnetic parameters $\xi_\nu^0(\mathrm{Fe})$, $\xi_\nu^0(\mathrm{Co})$, $\nu=\alpha,\beta$, as functions of temperature for the same set of values as those in Fig. 2.

C. $\Theta_M < \Theta_0$

Results for alloys with $\Theta_M < \Theta_0$ are shown in Figs. 5 and 6. In Fig. 5 we show the temperature dependence of the order parameters η, η_0, $\bar{\xi}$, and $\bar{\xi}^0$. Results for the surface concentration are shown also. In Fig. 6, we present the results for x_0, η_0, and $\bar{\xi}^0$ as function of Δ_{eff} and for several temperatures. The common parameters used are $J_{AA}=1$, $J_{AB}=0.5$, $J_{BB}=2$, $x=0.5$, $W_C=1.2$, and $W_{\mathrm{eff}}=0.7$.

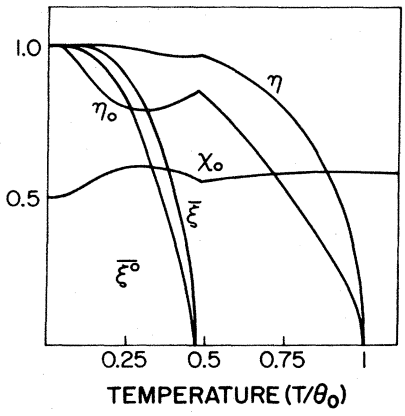

FIG. 5. Temperature dependence of η, η_0, $\bar{\xi}$, $\bar{\xi}^0$, and x_0 for an alloy with $\Theta_M < \Theta_0$. The parameters used are $x=0.5$, $J_{AA}=1$, $J_{BB}=2$, $J_{AB}=0.5$, $W_C=1.2$, $W_M=-0.5$, $\Delta_C=1$, and $\Delta_M=0.5$.

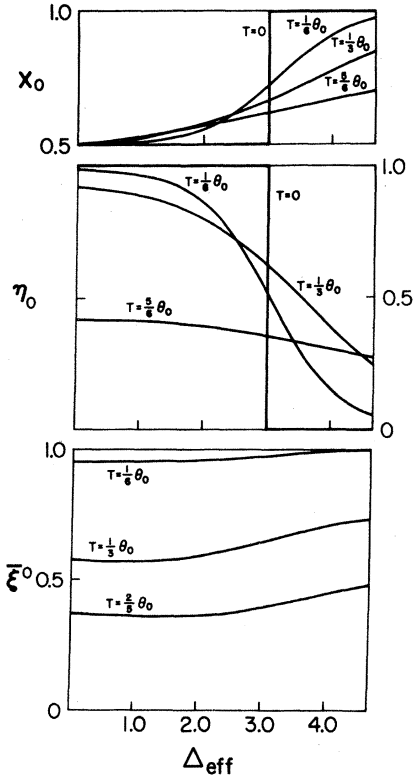

FIG. 6. Surface concentration x_0, long-range order parameter η_0 and average magnetization $\bar{\xi}^0$ as functions of Δ_{eff} and for several values of Δ_{eff}. The set of values used for the parameters correspond to those of Fig. 5.

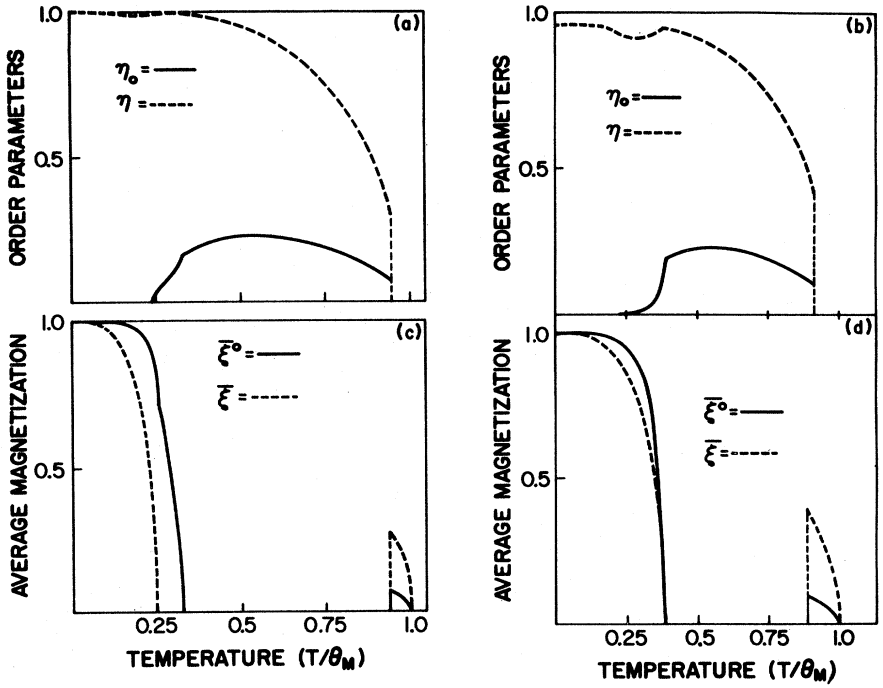

FIG. 7. Temperature dependence of η_0, η, $\bar{\xi}^0$, and $\bar{\xi}$ for an alloy with $J_{AB} << J_{AA}$ and J_{BB} and $\Theta_0 < \Theta_M$. The common parameters of these two figures are $x = 0.5$, $J_{AA} = 1$, $J_B = 2$, $W_C = 1$, $W_M = -0.25$, $\Delta_C = 4$, and $\Delta_M = -0.625$. The only different parameter, J_{AB}, was taken as 0.25 and 0.35 for the left and right figures correspondingly.

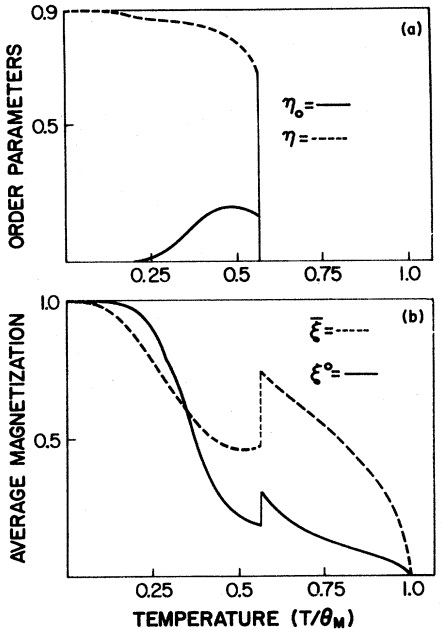

FIG. 8. Temperature dependence for η_0, η, $\bar{\xi}^0$, and $\bar{\xi}$ for an alloy with $J_{AB} << J_{AA}$ and J_{BB} and $\Theta_0 < \Theta_M$. This alloy is characterized by $x = 0.45$, $J_{AA} = 1$, $J_{BB} = 2$, $J_{BB} = 2$, $J_{AB} = 0.25$, $W_C = 1$, $W_M = -0.625$, $\Delta_C = 4$ and $\Delta_M = -0.25$.

D. $J_{AB} << J_{AA}, J_{BB}$ and $\Theta_0 < \Theta_M$

As mentioned in Sec. II C, in this case the system might become paramagnetic in the low-temperature regime. We show results for the surface parameters $\bar{\xi}^0$ and η_0 as functions of temperature in Figs. 7 and 8 for several sets of parameters. The bulk results are shown also for comparison. The temperature dependence of the surface concentration corresponding to the set of values used in Figs. 7 and 8 are shown in Fig. 9.

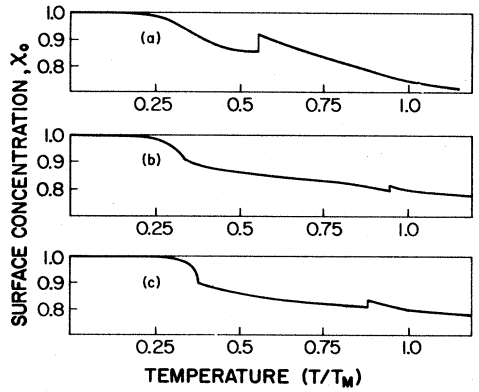

FIG. 9. Surface concentration x_0 as a function of temperatures for the three alloys of Figs. 7 and 8. (a), (b), and (c) correspond to the alloys in Figs. 9, 8(a), and 8(b).

E. Relaxation of the atomic interaction energies and of the Ising exchange integrals at the surface

The atomic interaction energies as well as the Ising exchange integrals at the surface might in general, be different from their bulk values. In particular if we assume that the interaction energies and the Ising exchange integrals change near the surface in the following way:

$$J_{II'}^{nm}=\begin{cases}\beta^2 J_{II'}\ , & n=m=0\\ \beta J_{II'}\ , & n=0,\ \ n=1\\ J_{II'}\ , & \text{otherwise}\ ,\end{cases} \tag{3.15}$$

$$U_{II'}^{nm}=\begin{cases}\alpha^2 U_{II'}\ , & n=m=0\\ \alpha U_{II'}\ , & n=0,\ \ m=1\\ U_{II'}\ , & \text{otherwise}\end{cases} \tag{3.16}$$

$(I,I'=A,B)$, the critical values Δ_1 and Δ_2 are given now by

$$\Delta_1^*=\begin{cases}\dfrac{Z_0(1+\gamma_0\gamma_1)+Z_1(2+3\gamma_0)-4x\gamma_0 Z_1}{D}\ , & x>\frac{1}{2}\\ \gamma_0\dfrac{Z_1+\gamma_1 Z_0}{D}\ , & x=\frac{1}{2}\\ -\dfrac{Z_1(2-\gamma_0)+Z_0(1-\gamma_1\gamma_0)}{D}\ , & x<\frac{1}{2}\ ,\end{cases} \tag{3.17}$$

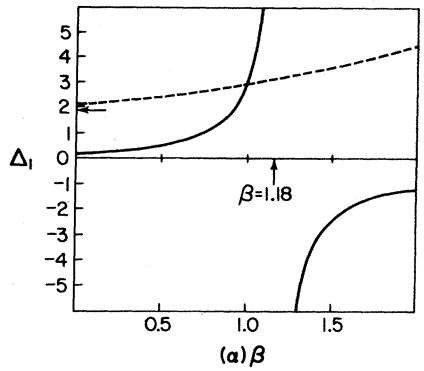

FIG. 10. Limiting values Δ_1 as a function of $\alpha(\beta)$, broken curve (continuous curve) (see text), for the parameters of the FeCo system. For each curve we took $\beta(\alpha)=1$. The horizontal arrow marks the value of Δ_{eff} for FeCo and $\alpha=\beta=1$. The vertical arrow marks the value of β at which the divergence occurs.

and

$$\Delta_2^*=\begin{cases}-\dfrac{Z_1(2-\gamma_0)+Z_0(1-\gamma_0\gamma_1)}{D}\ , & x>\frac{1}{2}\\ \Delta_1^*\ , & x=\frac{1}{2}\\ \dfrac{Z_1(2-\gamma_0+4x\gamma_0)+Z_0(1+\gamma_1\gamma_0)}{D}\ , & x<\frac{1}{2}\ ,\end{cases} \tag{3.18}$$

where

$$D=Z-\gamma_3(Z_1+Z_0\gamma_2)\ , \tag{3.19}$$

$$\gamma_0=\frac{\beta W_C+\alpha W_M}{W_C+W_M},\quad \gamma_1=\frac{\beta^2 W_C+\alpha^2 W_M}{\beta W_C+\alpha W_M}\ , \tag{3.20}$$

$$\gamma_2=\frac{\beta^2\Delta_C W_C-\alpha^2\Delta_M W_M}{\beta\Delta_C W_C-\alpha\Delta_M W_M},\quad \gamma_3=\frac{\beta\Delta_C W_C-\alpha\Delta_M W_M}{\Delta_C W_C-\Delta_M W_M}\ ,$$

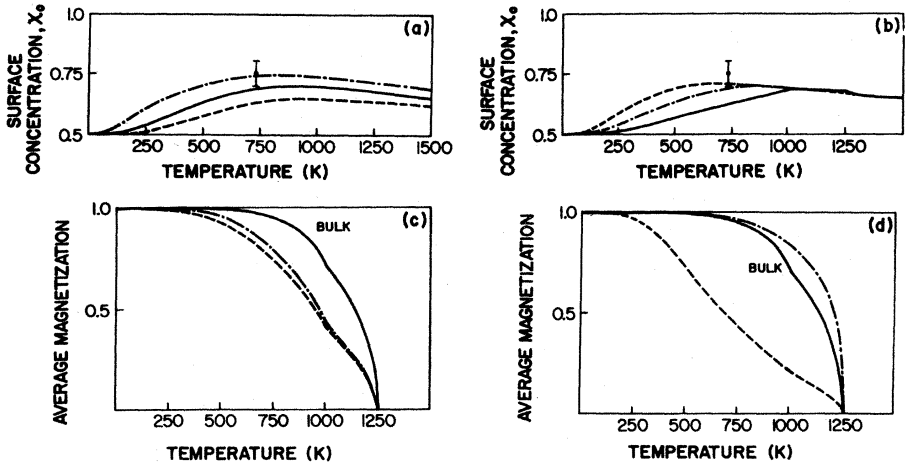

FIG. 11. Temperature dependence of x_0, $\bar{\xi}^0$, and $\bar{\xi}$ for several values of α and β and for the $Fe_{0.5}Co_{0.5}$ system. The left figures correspond to $\alpha=1$, $\beta=0.95$ (−·−), $\beta=1$ (−), and $\beta=1.05$ (− − −). The right figures correspond to $\beta=1$, $\alpha=0.7$ (− − −), $\alpha=1$ (− −), and $\alpha=1.4$ (−). The experimental results (Ref. 15) are shown by the bar at $T=725$ K.

In Fig. 10 we show Δ_1^* as a function of $\alpha(\beta)$ taking in each case $\beta(\alpha)=1$ and $x=0.5$. The set of parameters used correspond to the FeCo system. The value for Δ_{eff} with $\alpha=\beta=1$ and for this alloy is marked by the horizontal arrow. The divergence for the case of Δ_1^* as a function of β is marked by the vertical arrow and corresponds to the value that makes $D=0$.

Results for the concentration x_0 and the average magnetization $\bar{\xi}^0$ as functions of the temperature are presented in Fig. 11. The set of values correspond to the FeCo system and for the two cases (i) $\alpha=1$, $\beta=0.95$, 1, and 1.05 and (ii) $\beta=1$, $\alpha=0.7$, 1, and 1.4.

IV. DISCUSSION

A. General remarks

We have developed a theory for the surface effects in ordering alloys with two ferromagnetic components. It is a mean-field theory where only long-range-order effects were taken into account. Magnetism, spatial long-range order and segregation were considered on the same footing and the interplay between all these phenomena was studied for alloys with several bulk behaviors. The driving parameter at the surface is Δ_{eff} defined in Eq. (3.11). It contains chemical and magnetic contributions. As mentioned above, magnetism would tend to segregate the element I if $S_I^2 J_{II} < S_{I'}^2 J_{I'I'}$. As shown in Fig. 1, at $T=0$ we find that the surface layer might have different concentration and spatial and magnetic order than the bulk. For $x=0.5$ this occurs if $\Delta_{\text{eff}} > \Delta_1$ or $\Delta_{\text{eff}} < -\Delta_1$. For $x \neq 0.5$ the surface layer is always different from the bulk, it can be completely ordered, i.e., $x=0.5$, $\eta_0=1$ or completely segregated $x_0=0.1$, $\eta_0=0$. The magnetic order parameters $\xi_I^0(\nu)$ might also be different from the bulk values. However, in the case $S_A=S_B=\frac{1}{2}$, the average magnetization $\bar{\xi}^0$ would be the same and independent of Δ_{eff}.

For finite temperatures, we studied several cases. Figures 2–4 contain the results for an alloy with $\Theta_0 < \Theta_M$. Here we took Δ_C and $\Delta_M > 0$ but with $\Delta_C > \Delta_M$. The chemical effects would tend to segregate the element A in contrast to magnetism. In Fig. 2 the results for the temperature dependence of x_0 for several values of x are displayed. We see that the dominant effect is due to the chemical interactions and the element A is segregated over the whole range of temperatures, except for $x=0.5$ and $T=0$. The spatial order-disorder temperature T_0 is marked with an open arrow for a given concentration and the Curie temperature Θ_M is marked with a solid arrow. For $x<0.5$ we find that $x_0=0.5$ at $T=0$, decreases and has a minimum in the range $0<T<T_0$, increases up to a maximum at $T=T_0$, and then it decreases monotonically. For $x=0.5$, $x_0=0.5$ at $T=0$, increases to a maximum at $T=T_0$ and then decreases monotonically. For $x>0.5$, $x_0=1$ at $T=0$ and then decreases monotonically as a function of temperature. It is worth noticing the behavior of x_0 for $x=0.505$. Results for η_0 and $\bar{\xi}^0$ for the same system and for the same bulk concentrations are shown in Fig. 3. The bulk results are shown also for comparison. In general, the average magnetization at the surface $\bar{\xi}^0$ is smaller than the bulk one but with no drastic changes. The spatial long-range order on the other hand might be very different for $x \neq 0.5$. For example, for $x=0.505$, $\eta_0=0$ at $T=0$, then it increases up to a maximum and it decreases again and vanishes at $T=T_0$. The magnetic order parameters at the surface are shown in Fig. 4 for the same set of parameters used in Figs. 2 and 3. They might be also very different from the bulk ones. The two upper figures correspond to $x=0.3$ and 0.5. In these two cases $x_0=\frac{1}{2}$ at $T=0$ and therefore $\xi_\alpha^0(A)=\xi_\beta^0(B)=1$, $\xi_\alpha^0(B)=\xi_\beta^0(A)=0$. Above T_0 the spatial long-range order disappears and $\xi_\alpha^0(I)=\xi_\beta^0(I)$, $I=A,B$. The lower figures correspond to $x=0.505$ and $x=0.6$. Here, at $T=0$, $x_0=1$, $\xi_\alpha^0(A)=\xi_\beta^0(A)=1$ and $\xi_\alpha^0(B)=\xi_\beta^0(B)=0$. At finite temperatures, the ξ^0's associated with the element. A decrease and the ones associated with the element B do the opposite. These parameters are different whenever $\eta_0 \neq 0$.

We have considered also the case when $\Theta_M < \Theta_0$. In Fig. 5 we show the results for an alloy characterized by $x=0.5$, $J_{AA}=1$, $J_{BB}=2$, $J_{AB}=0.5$, $W_C=1.2$, $W_M=-0.5$, $\Delta_M=0.5$, and $\Delta_C=1$. This system is ferromagnetic at low temperatures. We see from Fig. 5 that η_0 and x_0 are strongly influenced by this phenomenon. We show in Fig. 6 how x_0, η_0, and $\bar{\xi}^0$ depend on Δ_{eff} and for several values of T. The system becomes paramagnetic at $T=\frac{5}{6}\Theta_0$.

A more interesting case is the one with $\Theta_0 < \Theta_M$ and $J_{AB} << J_{AA}, J_{BB}$. As discussed somewhere else,[11] these systems present the following sequence of phases as the temperature is increased: ordered ferromagnet, ordered paramagnet, disordered ferromagnet, and disordered paramagnet. The low-temperature paramagnetic phase is due to the fact that the system is spatially highly ordered and the ferromagnetic coupling between dissimilar atoms is small. The system can take advantage of the strong exchange interaction only if there is sufficient disorder to permit A-A and B-B pairs to exist as nearest neighbors. This is the ferromagnetism that appears at high temperatures. In Fig. 7(a) we present the results for η_0 and $\bar{\xi}^0$ as functions of T for an alloy with, $J_{AA}=1$, $J_{BB}=2$, $J_{AB}=0.25$, $x=0.5$, $W_C=1$, $W_M=-0.625$, $\Delta_C=4$, and $\Delta_M=-0.25$. We see that $\eta_0 \simeq 0$ for the low-temperature ferromagnetic region as a consequence of the high segregation $x_0 \simeq 1$. Therefore, the surface behaves like a two-

dimensional magnetic system with coupling constant J_{AA} ($>> J_{AB}$) and stays ferromagnetic at temperatures above the first bulk Curie temperature. This effect disappears if we increase J_{AB} as shown in Fig. 7(b). In this case the value for $J_{AB}=0.35$. In these two examples the surface magnetization in the low-temperature phase is stronger than the corresponding to the bulk. This situation is inverted at high temperatures where segregation has diminished. The results for x_0 as a function of T are shown in Figs. 9(b) and 9(c). In Fig. 8 we present results for the case where the intermediate paramagnetic phase disappears. The set of values used is the same as in Fig. 7 but with $x=0.45$. The segregation in this alloy is also very strong [see Fig. 9(a)] and $\eta_0 \to 0$ as $T \to 0$. The surface magnetization at low temperatures is also in this case stronger than the bulk but as the x_0 decreases the difference $\bar{\xi}^0 - \bar{\xi}$ becomes smaller and changes sign at higher temperatures.

We studied also relaxation effects at the surface. We assumed that the atomic interaction energies and the Ising exchange integrals change according to Eqs. (3.15) and (3.16). Under this assumption, the effect produced by the relaxation is to modify the internal energy in a way that can be interpreted as if the number of nearest neighbors of atoms at the surface would be modified. This can be seen from Eq. (3.19) where $\gamma_3 Z_1$ and $\gamma_2\gamma_3 Z_0$ could be taken as effective numbers Z_1^* and Z_0^* and $Z_{\text{sup}}^* = Z_1^* + Z_0^*$ as the effective number of nearest neighbors of atoms at the surface. When this number is equal to the bulk one, then it is not possible to distinguish the surface from the bulk since in our theory the surface enters only by the difference in coordination number. This is why in that case $D=0$ and Δ_1^* and Δ_2^* diverge as shown in Fig. 10. For $x=0.5$, it does not matter how big is Δ_{eff}, the only solution at $T=0$ is the bulk ordered situation. For values of $\alpha(\beta)$ such that $Z_{\text{sup}}^* > Z$, the situation of surface and bulk is inverted and for $\Delta > 0$ the surface would be enriched by B atoms. This is why Δ_1^* becomes negative for values of β such that $Z_{\text{sup}}^* > Z$.

In Fig. 11 we show the results for the concentration x_0 and the average magnetization $\bar{\xi}^0$ as functions of the temperature for several values of α and β. From Figs. 10 and 11 we can see that changes in the U's are much more important as compared with those of the J's.

B. Fe_xCo_y system

The Fe_xCo_y system corresponds to the kind of systems described in Sec. III B with $\Theta_0 < \Theta_M$. This system was studied in detail and the results are shown in Figs. 2–4, 10, and 11.

Those results were discussed above. Here we just want to stress the importance of this system to distangle the very interesting interplay of spatial order-disorder phenomena and magnetism. Here, we have included the only experimental results available (x_0 for $x=0.5$ and $T=725$ K). Experiments performed at lower temperatures in this alloy would be desirable to check the validity of our theory.

ACKNOWLEDGMENTS

We are grateful to Professor R. D. Parks, Professor L. M. Falicov, Professor K. H. Bennemann, and Professor C. E. T. Gonçalves da Silva for stimulating discussions. This work was supported in part by Dirección General de Investigación Científica y Superación Académica de la Secretaría de Educación Pública (México) under Contract No. 79-04-285 and by Programa Regional de Desarrollo Científico of the Organización de Estados Americanos.

[1] J. L. Morán-López and L. M. Falicov, Phys. Rev. B 18, 2542 (1978).
[2] J. L. Morán-López and L. M. Falicov, Phys. Rev. B 18, 2549 (1978).
[3] V. Kumar, C. E. T. Gonçalves da Silva, and J. L. Morán-López, Phys. Rev. B 23, 2752 (1981) (preceding paper).
[4] J. L. Morán-López and L. M. Falicov, Phys. Rev. B 19, 1470 (1979); 20, 3900 (1979).
[5] J. Urías and J. L. Morán-López, Surf. Sci. (in press).
[6] C. R. Housaka, J. Phys. Chem. Solids 24, 95 (1963).
[7] T. W. McDaniel and C. W. Foiles, Solid State Commun. 14, 835 (1974).
[8] F. Brouers and A. V. Vedyayev, Solid State Commun. 9, 1521 (1971).
[9] A. Theumann, J. Phys. C 7, 2328 (1974).
[10] J. L. Morán-López and L. M. Falicov, Solid State Commun. 31, 325 (1979).
[11] J. L. Morán-López and L. M. Falicov, J. Phys. C 13, 1715 (1980).
[12] R. H. Fowler and E. A. Guggenheim, *Statistical Thermodynamics* (Oxford University, London, 1939).
[13] M. Hansen, *Constitution of Binary Alloys* (McGraw-Hill, New York, 1958).
[14] J. A. Oyedelle and M. F. Collins, Phys. Rev. B 16, 3208 (1977).
[15] J. L. Morán-López and H. Wise, Appl. Surf. Sci. 4, 93 (1980).